WEP Warwick Evans Publishing

International Journal of Natural Resources and Environmental Studies

ISSN: 3006-2012 (Print), ISSN: 3006-0834 (Online) | Volume 8, Number 3, Year 2026
DOI: https://doi.org/10.62051/ijnres.v8n3.02
Journal homepage: https://wepub.org/index.php/IJNRES/index

Spatiotemporal Evolution of Urban Carbon Emissions Based on Night-Time Light Data: A Case Study of Yichang, China

Yiwen Zhang

School of Architecture and Art, Central South University, Changsha, Hunan, China

ABSTRACT

Urban spatial patterns significantly influence carbon emissions, yet research on their precise correlation at the micro-scale remains insufficient. This study integrates DMSP-OLS nighttime light data (2000–2011) and SNPP-VIIRS data (2012–2020) to simulate the spatial distribution of carbon emissions in the main urban area of Yichang. A linear regression model was established between the corrected nighttime light index and the calculated carbon emissions derived from energy consumption data The results indicate a strong positive correlation between night-time light intensity and carbon emissions. Furthermore, the carbon emission center is predominantly concentrated in the Xiling District and diffuses toward the suburbs. Based on these findings, this study proposes urban spatial management strategies aligned with compact city development, including decentralizing core functions, intensive land utilization, and expanding green spaces to facilitate low-carbon transition and sustainable urban development.

KEYWORDS

Carbon emissions; Night-time light data; Spatial evolution; Compact city.

1. INTRODUCTION

With the escalating threats of global climate change, achieving carbon neutrality has emerged as a crucial strategy for climate mitigation. China is currently experiencing rapid urbanization, and the central government places a high priority on the "low-carbon development" of cities[1]. From promoting the "reform of the ecological civilization system" to collaboratively advancing carbon reduction, pollution control, green expansion, and economic growth, China has been consistently exploring a low-carbon development path tailored to its national conditions[2].

On September 22, 2020, at the 75th United Nations General Assembly, China announced its commitment to peak carbon emissions by 2030 and achieve carbon neutrality by 2060[3]. The Central Economic Work Conference in December 2021 further clarified the transition from dual control over energy consumption to dual control over both the total amount and intensity of carbon emissions[4]. Consequently, carbon reduction has become a societal priority. Cities, as the primary spatial carriers of human activities, consume vast amounts of fossil fuels; their total carbon emissions have increased significantly since the Industrial Revolution, causing substantial negative impacts on global biodiversity and environmental protection. Against this backdrop, understanding the spatial distribution of urban carbon emissions and its relationship with urban spatial morphology is a critical strategic requirement for promoting low-carbon transitions and sustainable development[5].

Research on low-carbon development emerged earlier in Western contexts. The concept of a "low-carbon economy," first introduced in 2003, marked the genesis of related development philosophies, which subsequently gained global traction[2]. Building upon this, Japanese scholars proposed the

concept of a "low-carbon society" in 2007, sparking extensive academic discourse[6]. For instance, scholars conducted systematic evaluations of "low-carbon communities," revealing their positive ecological impacts, while Tulin investigated the socio-economic influences on residents' consumption choices and renewable energy usage in South Africa, summarizing the challenges faced by local low-carbon economic development.

Conversely, domestic research on "low-carbon cities" in China, while initially nascent, has deepened significantly following the introduction of related policies. In recent years, numerous scholars have explored the spatiotemporal evolution of urban carbon emissions[7]. For example, Li, J [8] analyzed the spatial-temporal evolution and influencing factors of carbon emissions in Chinese urban agglomerations, finding that industrial structure and international trade levels significantly impact emissions. H. Huan[9] utilized the Super-SBM model to predict the evolving patterns of China's urban carbon emission performance, noting a stable upward trend and geographical correlations. Furthermore, Q. Meng[10] examined the dynamic transitions and convergence trends of urban carbon emission intensity in China, highlighting significant positive spatial correlations[8].

Existing literature indicates that urban spatial patterns significantly influence carbon emissions; however, research focusing on the precise correlation between urban carbon emissions and micro-spatial patterns remains insufficient. This study integrates DMSP-OLS nighttime light data (2000–2011) and SNPP-VIIRS data (2012–2020). A cross-calibration process was conducted to ensure temporal consistency between the two datasets. Focusing on the main urban area of Yichang as a case study, a carbon emission assessment model based on night-time lighting data is established to reveal the spatiotemporal variation laws of carbon emissions at a micro-scale. Simultaneously, it quantitatively characterizes the intrinsic relationship between the urban spatial environment and carbon emissions, proposing optimized regulatory measures to facilitate urban low-carbon transition and green development.

With the refinement of urban night-time light data in recent years, its application scope has gradually expanded. To better reflect the temporal and spatial distribution of urban "carbon emissions" and overcome the limitations of accuracy and timeliness in existing methodologies, researchers have increasingly utilized night-time lighting data. Initial explorations in the 1980s established a robust linear relationship between night-time lighting data and energy consumption, leading to its widespread adoption in carbon emission research. While international scholars established high-precision inversion models early on, domestic application in China predominantly began post-2016. It is worth noting that while night-time lighting data fills gaps in spatial research, it is most applicable to cities dominated by service and light industries, rather than heavily polluted industrial regions.

2. METHODS

2.1. Study Area

Yichang is located in the southwestern part of Hubei Province, serving as a transitional zone between the upper and middle reaches of the Yangtze River. The study area focuses on the main urban area of Yichang, encompassing five municipal districts: Yiling, Xiling, Wujiagang, Dianjun, and Xiaoting (Figure 1). The total evaluated area covers 4,246.51 square kilometres.

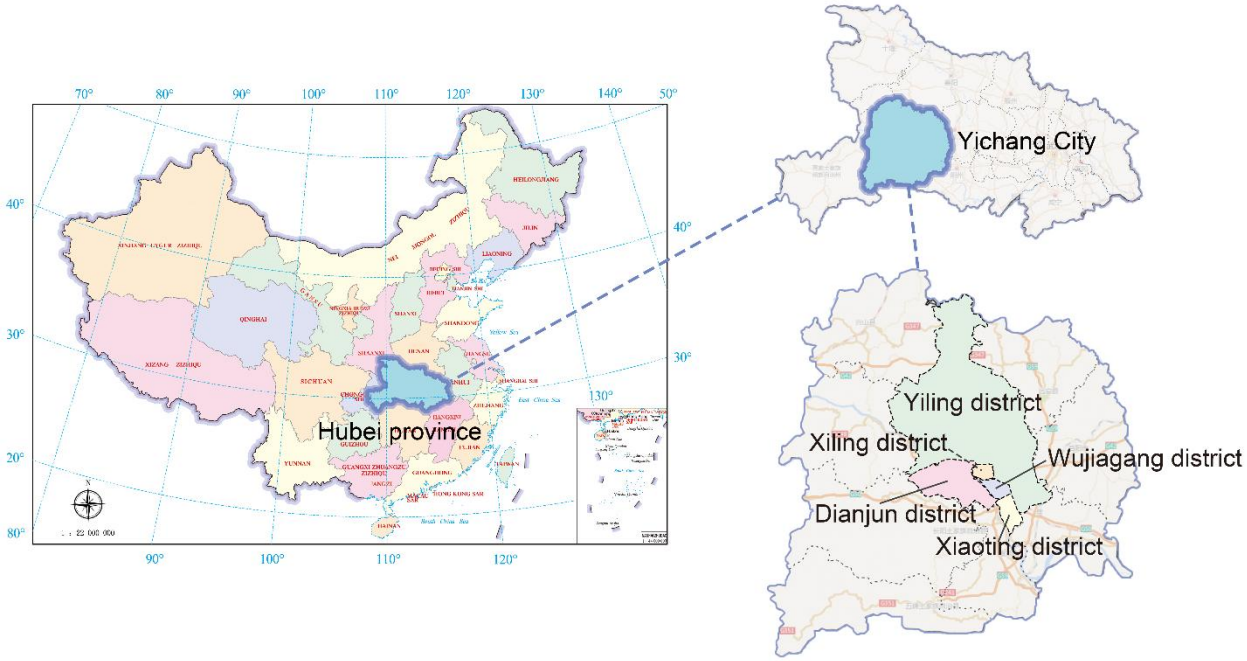

Figure 1. Study Area

2.2. Data sources and preprocessing

2.2.1. Land Use Data.

The land use patterns of Yichang from 2000 to 2020 are illustrated in the corresponding land use maps (Figure 2)

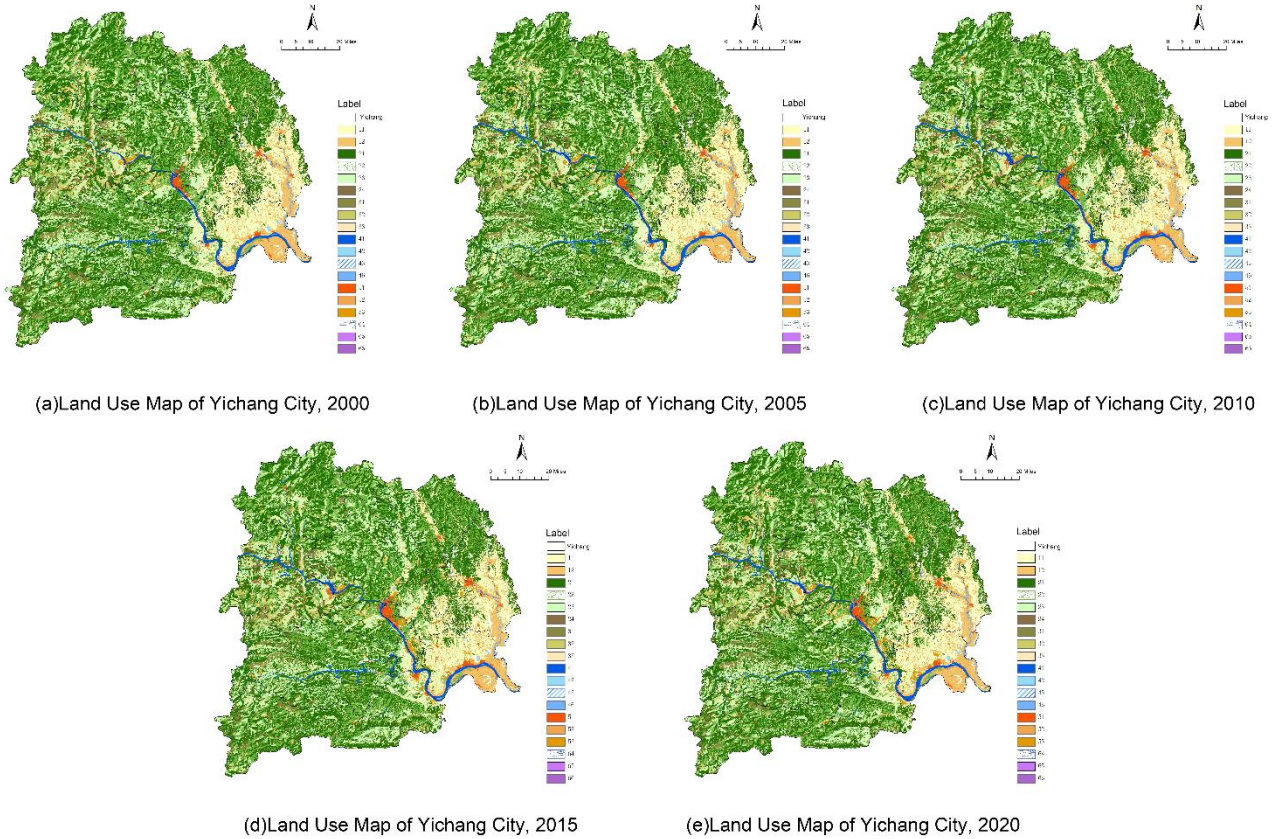

Figure 2. Land Use Map of Yichang (2000-2020)

2.2.2. Night-Time Light Data.

DMSP-OLS night-time light data (2000–2011) and SNPP-VIIRS data (2012–2020) were used in this study.The "Median-Low Threshold Method" was utilized for data processing. This method, proposed by Zhong Liang in his study on denoising SNPP-VIIRS night-time light imagery, primarily involves median filtering and low-threshold denoising. The light data of Yichang contains minor background noises caused by cloud reflection, auroras, and surface reflection, which cannot be entirely eliminated through standard median filtering and calibration. These isolated noise sources, especially those at the edges of the images, significantly impact measurement accuracy and must be removed. During the processing of the light image data, a suitable two-dimensional template was selected to divide the acquired raster data into 3×3 or 5×5 regions (or other odd-numbered regional templates), and the raster grayscale values were sorted by magnitude. The output model for the two-dimensional median filtering is as follows:

$$g(x,y) = med\{f(x-y, y-l), (k,l) \in W\} \quad (1)$$

where $f(x-y)$ and $g(x,y)$ represent the original and processed images, respectively; W denotes the two-dimensional raster template; and k and l represent the corresponding raster row and column numbers. To ensure temporal consistency, inter-calibration was conducted between DMSP-OLS and VIIRS datasets. The night-time light distributions for the years 2000 to 2020 are shown in Figure 3.

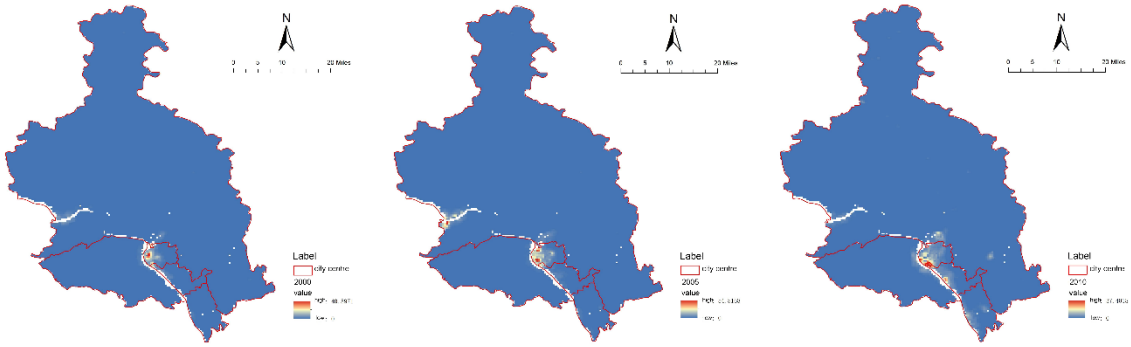

(a)Night-time Light Spatial Distribution Map 2000 (b)Night-time Light Spatial Distribution Map 2005 (c)Night-time Light Spatial Distribution Map 2010

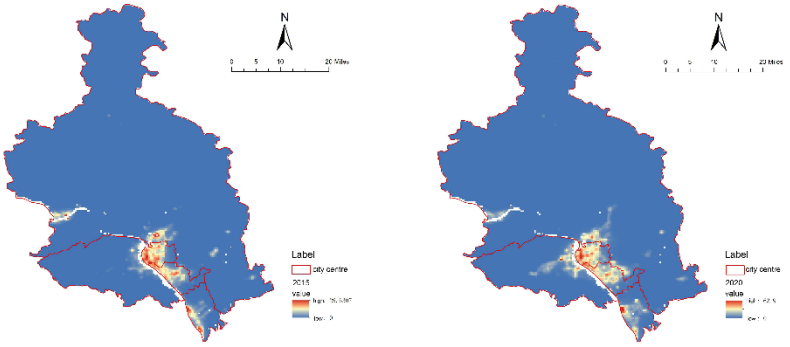

(d)Night-time Light Spatial Distribution Map 2015 (e)Night-time Light Spatial Distribution Map 2020

Figure 3. Night-time Light Spatial Distribution Characteristics Map of Yichang (2000–2020)

2.2.3. Land Use Area Statistics.

The statistical areas for various land use types in Yichang from 2000 to 2020 were systematically calculated. Specific parameters for cultivated land, forest land, grassland, water bodies, construction land, and unutilized land (bare land) are detailed in the aggregated statistics(Table 1).

Table 1. Land Use Area Statistics of Yichang (2000-2020)

Year	Land Use Type	Unit	value
2000	Arable land area	hm²	4655611
	Forest area	hm²	16917889
	Grassland area	hm²	981606
	Water area	hm²	638217
	Construction land area	hm²	406275
	Area of unutilised land (bare ground)	hm²	713
2005	Arable land area	hm²	4631150
	Forest area	hm²	16854157
	Grassland area	hm²	978459
	Water area	hm²	716740
	Construction land area	hm²	419327
	Area of unutilised land (bare ground)	hm²	703
2010	Arable land area	hm²	4445943
	Forest area	hm²	16918495
	Grassland area	hm²	974498
	Water area	hm²	727281
	Construction land area	hm²	533702
	Area of unutilised land (bare ground)	hm²	805
2015	Arable land area	hm²	4360501
	Forest area	hm²	16866145
	Grassland area	hm²	973476
	Water area	hm²	727039
	Construction land area	hm²	672405
	Area of unutilised land (bare ground)	hm²	808
2020	Arable land area	hm²	4506873
	Forest area	hm²	16757973
	Grassland area	hm²	977334
	Water area	hm²	718744
	Construction land area	hm²	638940
	Area of unutilised land (bare ground)	hm²	719

2.2.4. Statistical Yearbook Data.

Due to the availability constraints of the Yichang Municipal Statistical Yearbook (which began publication in 2010) and the missing data for the years 2000 and 2005 in the Hubei Provincial Statistical Yearbook, data from three representative years—2010, 2015, and 2020—were selected for this study. The socio-economic, demographic, agricultural, and industrial energy consumption indicators for these years are comprehensively analyzed(Table 2).

Table 2. Statistical Yearbook Data (2010-2020)

Year	Sector	Indicator	Value
2010	Land use	Municipal administrative area (square kilometres)	21084
		Municipal district area (square kilometres)	/
	Population	Permanent resident population at year-end (in ten thousand persons)	398.84
		Urban population (in ten thousand)	202.42
		Rural population (in ten thousand)	196.42
		Urbanisation rate (ten thousand persons)	51.99%
	Economy	GDP (billion yuan)	2140.69
		Primary Industry (billion yuan)	240.81
		Secondary industry (billion yuan)	1295.24
		Tertiary sector (billion yuan)	1189.44
		Per capita GDP (yuan)	52673
	Agriculture	Total Agricultural Machinery Power (10,000 kilowatts)	260.66
		Effective irrigated area (thousand hectares)	59
		Rural electricity consumption (megawatt-hours)	77772
		Fertiliser application volume (ton)	365689
	Industry	Energy consumption of industrial enterprises above designated size (in ton of standard coal equivalent)	13001398
		Raw coal consumption (ton)	11994285
		Coke consumption (ton)	535622
		Crude oil consumption (ton)	3
		Fuel oil consumption (ton)	1568
		Petrol consumption (ton)	7465
		Kerosene consumption (ton)	1183
		Diesel consumption (ton)	31939
		Liquefied petroleum gas consumption (ton)	460
		Natural gas consumption (million cubic metres)	33153
2015	Land use	Municipal administrative area (square kilometres)	21084
		Municipal district area (square kilometres)	/
	Population	Permanent resident population at year-end (in ten thousand persons)	411.50
		Urban population (in ten thousand)	235.17
		Rural population (in ten thousand)	176.33
		Urbanisation rate (ten thousand persons)	57.15%
	Economy	GDP (billion yuan)	3384.80
		Primary Industry (billion yuan)	370.31
		Secondary industry (billion yuan)	1986.41
		Tertiary sector (billion yuan)	1028.08
		Per capita GDP (yuan)	82360
	Agriculture	Total Agricultural Machinery Power (10,000 kilowatts)	3182254
		Effective irrigated area (thousand hectares)	121.92
		Rural electricity consumption (megawatt-hours)	114864
		Fertiliser application volume (ton)	365844
	Industry	Energy consumption of industrial enterprises above designated size (in ton of standard coal equivalent)	14868226

		Raw coal consumption (ton)	14127228
		Coke consumption (ton)	505667
		Crude oil consumption (ton)	/
		Fuel oil consumption (ton)	19
		Petrol consumption (ton)	11174
		Kerosene consumption (ton)	1219
		Diesel consumption (ton)	35208
		Liquefied petroleum gas consumption (ton)	77
		Natural gas consumption (million cubic metres)	11346
	Land use	Municipal administrative area (square kilometres)	21084
		Municipal district area (square kilometres)	211
	Population	Permanent resident population at year-end (in ten thousand persons)	401.76
		Urban population (in ten thousand)	256.2
		Rural population (in ten thousand)	145.56
		Urbanisation rate (ten thousand persons)	63.77%
		GDP (billion yuan)	4261.42
		Primary Industry (billion yuan)	459.68
	Economy	Secondary industry (billion yuan)	1828.46
		Tertiary sector (billion yuan)	1973.28
		Per capita GDP (yuan)	106081
		Total Agricultural Machinery Power (10,000 kilowatts)	3207354
2020	**Agriculture**	Effective irrigated area (thousand hectares)	142.59
		Rural electricity consumption (megawatt-hours)	121560
		Fertiliser application volume (ton)	295065
		Energy consumption of industrial enterprises above designated size (in ton of standard coal equivalent)	11552997
		Raw coal consumption (ton)	10221342
		Coke consumption (ton)	1655
		Crude oil consumption (ton)	/
	Industry	Fuel oil consumption (ton)	1218
		Petrol consumption (ton)	4206
		Kerosene consumption (ton)	76
		Diesel consumption (ton)	28987
		Liquefied petroleum gas consumption (ton)	645
		Natural gas consumption (million cubic metres)	16902

2.3. Carbon Emission Calculation

2.3.1. Calculation Method for Carbon Emissions.

The empirical coefficient method was adopted to quantify carbon emissions. The calculation formula is constructed as follows:

$$C_I = \sum_{i=1}^{n} E_i f_i \quad (2)$$

where C_I represents the total carbon emissions; E_i refers to the energy consumption (converted into standard coal); f_i denotes the carbon emission coefficient of various energy sources; i indicates the specific type of energy; and n is the total number of industrial energy consumption types. Detailed carbon emission estimations for 2010, 2015, and 2020 are presented sequentially(Table 3).

Table 3. Carbon emissions (2010-2020)

Year	Energy type	Energy consumption	Standard coal conversion factor Kilograms of standard coal per kilogram	Carbon emission factor kg/kgce （m3/kg ce）	carbon emissions
2010	**Energy consumption of industrial enterprises above designated size (tonnes of standard coal equivalent)**	13001398	/	/	/
	Raw coal consumption (ton)	11994285	0.7143	0.7559	6476186.687
	Coke consumption (ton)	535622	0.9714	0.855	444859.2452
	Crude oil consumption (ton)	3	1.4286	0.5857	/
	Fuel oil consumption (ton)	1568	1.4286	0.6185	1385.467709
	Petrol consumption (ton)	7465	1.4714	0.5538	6082.939754
	Kerosene consumption (ton)	1183	1.4714	0.5714	994.6166667
	Diesel consumption (ton)	31939	1.4571	0.5921	27555.33744
	Liquefied petroleum gas consumption (ton)	460	1.7143	0.5042	397.6010276
	Natural gas consumption (10,000 cubic metres)	33153	1.2143	0.4483	18047.52149
	Other energy consumption	395720	1.228	0.5857	284617.4945
		Total(ton)			7260126.91
2015	**Energy consumption of industrial enterprises above designated size (tonnes of standard coal equivalent)**	14868226	/	/	/
	Raw coal consumption (ton)	14127228	0.7143	0.7559	7627846.586
	Coke consumption (ton)	505667	0.9714	0.855	419980.2098
	Crude oil consumption (ton)	/	1.4286	0.5857	/
	Fuel oil consumption (ton)	19	1.4286	0.6185	16.7881929
	Petrol consumption (ton)	11174	1.4714	0.5538	9105.26039
	Kerosene consumption (ton)	1219	1.4714	0.5714	1024.883953
	Diesel consumption (ton)	35208	1.4571	0.5921	30375.66362
	Liquefied petroleum gas consumption (ton)	77	1.7143	0.5042	66.55495462
	Natural gas consumption (10,000 cubic metres)	11346	1.2143	0.4483	6176.429849
	Other energy consumption	176288	1.228	0.5857	126793.3106
		Total(ton)			8221385.688
2020	**Energy consumption of**	11552997	/	/	/

industrial enterprises above designated size (tonnes of standard coal equivalent)				
Raw coal consumption (ton)	10221342	0.7143	0.7559	5518904.96
Coke consumption (ton)	1655	0.9714	0.855	1374.555285
Crude oil consumption (ton)	/	1.4286	0.5857	/
Fuel oil consumption (ton)	1218	1.4286	0.6185	1076.211524
Petrol consumption (ton)	4206	1.4714	0.5538	3427.306712
Kerosene consumption (ton)	76	1.4714	0.5714	63.89760496
Diesel consumption (ton)	28987	1.4571	0.5921	25008.50265
Liquefied petroleum gas consumption (ton)	645	1.7143	0.5042	557.5057887
Natural gas consumption (10,000 cubic metres)	16902	1.2143	0.4483	9200.953402
Other energy consumption	1277966	1.228	0.5857	919163.7547
	Total(ton)			6478777.648

2.3.2. Calculation Method for Carbon Sinks.

Similarly, the empirical coefficient method was employed for carbon sink estimation, obtained by multiplying the land use area by the corresponding empirical conversion coefficient. The quantitative relationship is expressed as:

$$V_s = \sum_{i=1}^{n} k_i S_i \quad (3)$$

where S_i represents the area of a specific land use type acting as a carbon sink; n is the total number of carbon sink land use types; and k_i is the carbon absorption coefficient corresponding to that specific land use type. Based on this, the carbon sinks for the distinct study years were tabulated(Table 4).

Table 4. Carbon sink volume (2010-2020)

Year	Land Use Type	Carbon sequestration coefficient value	Area	carbon sink capacity
2010	Arable land area	0.0007	444693	311.2851
	Forest area	0.0657	16918495	1111545.122
	Grassland area	0.0138	974498	13448.0724
	Water area	0.0402	727281	29236.6962
		Total		1154541.175
2015	Arable land area	0.0007	4360501	3052.3507
	Forest area	0.0657	16866145	1108105.727
	Grassland area	0.0138	973476	13433.9688
	Water area	0.0402	727039	29226.9678
		Total		1153819.014
2020	Arable land area	0.0007	4506873	3154.8111
	Forest area	0.0657	16757973	1100998.826
	Grassland area	0.0138	977334	13487.2092
	Water area	0.0402	718744	28893.5088
		Total		1146534.355

2.3.3. Spatial Differentiation Characteristics of Carbon Emissions.

To evaluate the spatial differentiation characteristics systematically, several core metrics were calculated, including total carbon emissions, carbon emission intensity, carbon emission per unit area, and per capita carbon emission(Table 5).

Table 5. Spatial Variation Characteristics of Carbon Emissions

Sector	Formula for calculation	Unit	value
Total carbon emissions	$C_I = \sum_{i=1}^{n} E_i f_i$ The aggregate of carbon emissions from all types of energy consumption	10,000 tonnes	647.8777648
Carbon emissions intensity	carbon emissions /GDP， Carbon emissions per unit of GDP	10,000 tonnes/10,000 yuan	0.152033305
Carbon emissions per unit area	carbon emissions / Land area	tonnes/hectare	0.274517695
Carbon emissions per capita	carbon emissions / Permanent resident population	tonnes/person	1.612598977

2.3.4. Landscape Pattern Index (Central Urban Area).

To quantify the spatial structural changes, landscape pattern indices—such as Patch Area (AREA), Largest Patch Index (LPI), Patch Density (PD), and Landscape Fragmentation—were calculated for the central urban area over the two-decade span (Table 6).

Table 6. Landscape Pattern Indices of Yichang Central Urban Area (2000-2020)

Year	Index Name	Unit	Value
2000	Area of Patch (AREA)	ha	214.0514
	Area of Patch Type (CA)	ha	969876.1800
	Maximum Patch Index (LPI)	%	56.3629
	Number of Patches (NP)	#	2306.0000
	Patch Density (PD)	#/100ha	0.2378
	Shape Index (SHAPE)		1.7898
	Fractal Dimension (FRAC)		1.0853
	Euclidean Nearest Neighbor Distance (ENN)		428.3134
	Aggregation Index (AI)		98.5618
	Cluster Cohesion Index (COH)		99.8702
	Perimeter-Area Ratio (PARA_MN)		268.3800
	Landscape fragmentation		0.6200
2005	Area of Patch (AREA)	ha	210.4344
	Area of Patch Type (CA)	ha	423183.6000
	Maximum Patch Index (LPI)	%	56.3028
	Number of Patches (NP)	#	2011.0000
	Patch Density (PD)	#/100ha	0.4752
	Shape Index (SHAPE)		1.8423
	Fractal Dimension (FRAC)		1.0892
	Euclidean Nearest Neighbor Distance (ENN)		460.5067
	Aggregation Index (AI)		96.9041
	Cluster Cohesion Index (COH)		99.8708
	Perimeter-Area Ratio (PARA_MN)		207.4910
	Landscape fragmentation		0.6634
2010	Area of Patch (AREA)	ha	208.8785

2015	Area of Patch Type (CA)	ha	423187.8300
	Maximum Patch Index (LPI)	%	55.7800
	Number of Patches (NP)	#	2026.0000
	Patch Density (PD)	#/100ha	0.4787
	Shape Index (SHAPE)		1.8527
	Fractal Dimension (FRAC)		1.0891
	Euclidean Nearest Neighbor Distance (ENN)		449.3724
	Aggregation Index (AI)		96.8636
	Cluster Cohesion Index (COH)		99.8633
	Perimeter-Area Ratio (PARA_MN)		209.4725
	Landscape fragmentation		0.6701
	Area of Patch (AREA)	ha	420.5881
	Area of Patch Type (CA)	ha	969876.1800
	Maximum Patch Index (LPI)	%	56.3629
	Number of Patches (NP)	#	2306.0000
	Patch Density (PD)	#/100ha	0.2378
	Shape Index (SHAPE)		1.7898
	Fractal Dimension (FRAC)		1.0853
	Euclidean Nearest Neighbor Distance (ENN)		428.3134
	Aggregation Index (AI)		98.5618
	Cluster Cohesion Index (COH)		99.8702
	Perimeter-Area Ratio (PARA_MN)		268.3800
	Landscape fragmentation		0.6200
2020	Area of Patch (AREA)	ha	420.5881
	Area of Patch Type (CA)	ha	423187.8300
	Maximum Patch Index (LPI)	%	56.2339
	Number of Patches (NP)	#	2304.0000
	Patch Density (PD)	#/100ha	0.5444
	Shape Index (SHAPE)		1.8413
	Fractal Dimension (FRAC)		1.0892
	Euclidean Nearest Neighbor Distance (ENN)		392.951
	Aggregation Index (AI)		96.7100
	Cluster Cohesion Index (COH)		99.8566
	Perimeter-Area Ratio (PARA_MN)		235.7157
	Landscape fragmentation		0.6669

3. SPATIOTEMPORAL CHARACTERISTIC ANALYSIS OF CARBON EMISSIONS IN YICHANG

3.1. Correlation and Fitting Analysis Between Night-Time Light Data and Carbon Emissions.

Based on the SNPP-VIIRS night-time light data spanning five intervals between 2000 and 2020 (Figure 4), the spatial distribution characteristics of night-time light in Yichang were obtained using mathematical integer processing in GIS. Employing the GIS grid spatial index function, the main urban area was divided into 400m × 400m grids. The total grayscale value of night-time light increased from 1,879 in 2000 to 17,885 in 2020. The accelerated growth rate observed between 2010 and 2020 reflects the rapid urban expansion during this decade. By fitting the night-time light grayscale values with corresponding carbon emission statistics in SPSS, a robust linear regression model was established. The results yielded a Pearson correlation coefficient of 0.923($p < 0.01$) and an adjusted R^2 of 0.882, showing a significant correlation at the 0.01 level. This strong linear

relationship demonstrates the high feasibility of utilizing night-time light data to simulate urban carbon emissions. A logarithmic model was also tested; however, the linear model demonstrated superior explanatory power (higher adjusted R^2).

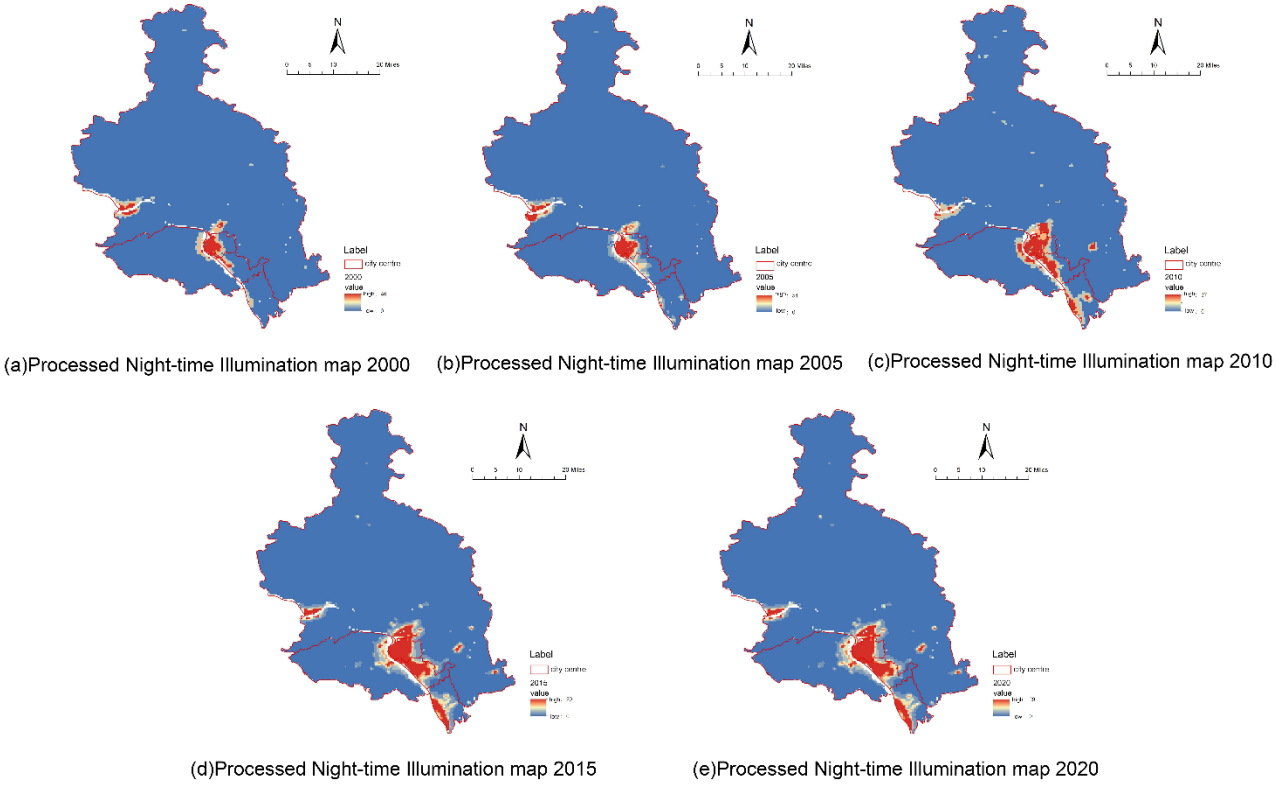

(a)Processed Night-time Illumination map 2000 (b)Processed Night-time Illumination map 2005 (c)Processed Night-time Illumination map 2010

(d)Processed Night-time Illumination map 2015 (e)Processed Night-time Illumination map 2020

Figure 4. Processed Night-time Light Spatial Distribution Characteristics Map of Yichang (2000–2020)

3.2. Temporal Evolution Analysis of Carbon Emissions.

Analyzing temporal variations enables urban planners to identify developmental trends and formulate sustainable strategies. The peak carbon emission values within the study area exhibited dynamic fluctuations over the two decades: 406,000 tons in 2000, peaking at 629,000 tons in 2020. Notably, Yichang's carbon emissions increased steadily from 2010 to 2015 (reaching 8.22 million tons city-wide) but experienced a significant decline by 2020 (dropping to 6.48 million tons). This inflection point effectively mirrors the positive impacts of the "13th Five-Year Plan," highlighting the city's successful implementation of green development and ecological planning concepts to mitigate carbon emissions.

3.3. Spatial Evolution Analysis of Carbon Emissions.

Spatially, the carbon emission center is predominantly concentrated in the Xiling District and diffuses outwards to the suburbs. Analyzing the administrative districts reveals that Xiling District, Wujiagang District, and southern Yiling District exhibit relatively high total carbon emissions, whereas Xiaoting District, Dianjun District, and the majority of Yiling District show significantly lower emissions. This spatial heterogeneity aligns perfectly with the economic and demographic concentration in the urban core, indicating that the highest brightness peaks in night-time light—and consequently, the highest carbon emissions—are tightly bound to the most developed urban sectors.

4. URBAN SPATIAL ENVIRONMENT MANAGEMENT MEASURES FOR CARBON REDUCTION

In the pursuit of sustainable development, promoting a "compact city" is a vital strategy. However, a compact city does not imply blind high-density development; rather, it emphasizes intensive land use, energy reduction, optimized transit, and pollution mitigation. As a "Type I large city," Yichang's current political and economic epicenter is highly concentrated in Xiling District. To adapt to future development, the city must transition from a "monocentric" pattern to a "polycentric and compact" spatial layout.

By integrating the resources of Xiling, Wujiagang, and southern Yiling districts, Yichang should establish new regional development hubs. Dispersing certain urban functions to surrounding areas will alleviate traffic congestion and population pressure in the primary core. Furthermore, upgrading public transportation infrastructure, particularly the Bus Rapid Transit (BRT) system, is essential to strengthen connectivity between these newly formed sub-centers and promote a jobs-housing balance.

In alignment with the "Yichang Territorial Spatial Master Plan (2021-2035)," the city aims to become a paradigm of ecological conservation along the Yangtze River and a capital of clean energy. Coordinating urban land use ensures the rational allocation of land resources. Intensive land utilization minimizes unnecessary development, curtails urban sprawl, and enhances the efficiency of public services and transit hubs, thereby reducing overall transportation-related carbon emissions.

Advancing compact city models requires highly efficient land utilization, which includes promoting green building designs, high-efficiency construction materials, and renewable energy management systems. Simultaneously, urban planners should strategically utilize fragmented or "leftover" urban plots to construct pocket parks and street-corner green spaces. These micro-green spaces are crucial for absorbing carbon dioxide, improving local air quality, regulating the urban microclimate, and mitigating stormwater runoff. This strategy not only enhances the quality of life but also directly contributes to the city's overall carbon sink capacity, as quantified in Section 2.3.2.

5. CONCLUSION

In conclusion, this study validates the feasibility of using SNPP-VIIRS night-time light data to assess urban carbon emissions. The spatiotemporal analysis of Yichang demonstrates a strong correlation between economic activity, as proxied by nighttime light intensity, and carbon emissions. Transitioning towards a polycentric, compact urban structure—complemented by intensive land use and the strategic expansion of green infrastructure—provides a viable pathway for Yichang, and similar rapidly urbanizing cities, to achieve low-carbon development and meet critical carbon neutrality targets.

REFERENCES

[1] W. Xia, Y. Ma, Y. Gao, Y. Huo, and X. Su, "Spatial-temporal pattern and spatial convergence of carbon emission intensity of rural energy consumption in China," Environmental Science and Pollution Research, vol. 31, no. 5, pp. 7751-7774, 2024/01/01 2024, doi: 10.1007/s11356-023-31539-9.

[2] G. Ni, Y. Fang, M. Niu, L. Lv, C. Song, and W. Wang, "Spatial differences, dynamic evolution and influencing factors of China's construction industry carbon emission efficiency," Journal of Cleaner Production, vol. 448, p. 141593, 2024/04/05/ 2024, doi: https://doi.org/10.1016/j.jclepro.2024.141593.

[3] X. Luo, X. Jin, X. Liu, and Y. Zhou, "Decoding the dynamics and disparities of urban carbon intensity under the influence of land use and demographics from both global and local perspectives," Applied Geography, vol. 181, p. 103689, 2025/08/01/ 2025, doi: https://doi.org/10.1016/j.apgeog.2025.103689.

[4] Y. Sun, S. Zheng, Y. Wu, U. Schlink, and R. P. Singh, "Spatiotemporal Variations of City-Level Carbon Emissions in China during 2000–2017 Using Nighttime Light Data," Remote Sensing, vol. 12, no. 18, p. 2916doi: 10.3390/rs12182916.

[5] N. Ke, X. Lu, B. Kuang, and X. Zhang, "Regional disparities and evolution trend of city-level carbon emission intensity in China," Sustainable Cities and Society, vol. 88, p. 104288, 2023/01/01/ 2023, doi: https://doi.org/10.1016/j.scs.2022.104288.

[6] Y. Q. Wang and H. W. Zhang, "Spatiotemporal Transition, Convergence Trend, and Driving Factors of Urban Carbon Emission Intensity in China,", Huan Jing Ke Xue, vol. 46, no. 11, pp. 6722-6737, Nov 8 2025, doi: 10.13227/j.hjkx.202410060.

[7] C. Wu, H. Deng, H. Zhao, and Q. Xia, "Spatiotemporal evolution and convergence patterns of urban carbon emission efficiency in China," Humanities and Social Sciences Communications, vol. 12, no. 1, p. 675, 2025/05/15 2025, doi: 10.1057/s41599-025-04916-7.

[8] J. Li, X. Huang, H. Yang, X. Chuai, and C. Wu, "Convergence of carbon intensity in the Yangtze River Delta, China," Habitat International, vol. 60, pp. 58-68, 2017/02/01/ 2017, doi: https://doi.org/10.1016/j.habitatint.2016.12.012.

[9] H. Huan, L. Wang, and Y. Zhang, "Regional differences, convergence characteristics, and carbon peaking prediction of agricultural carbon emissions in China," Environmental Pollution, vol. 366, p. 125477, 2025/02/01/ 2025, doi: https://doi.org/10.1016/j.envpol.2024.125477.

[10] Q. Meng and C. Li, "Spatiotemporal evolutionary patterns and influencing factors of urban carbon emissions in China," Ecological Indicators, vol. 176, p. 113665, 2025/07/01/ 2025, doi: https://doi.org/10.1016/j.ecolind.2025.113665.